JOURNAL OF COMPUTATIONAL PHYSICS 100, 116–127 (1992)

A Direct Simulation Monte-Carlo Method for Cluster Coagulation

KURT LIFFMAN

Department of Mathematics, University of Melbourne, Parkville, Victoria 3052, Australia

Received December 27, 1989; revised July 3, 1991

A method for analyzing cluster coagulation is presented which relies on a Monte-Carlo analysis of individual particles as they interact and form clusters from a homogeneous, monodisperse medium. Four case studies are shown, three of which compare the results of the code to the known analytic solutions of the Smoluchowski equation and the fourth considers the cluster size spectrum obtained from a generalized analytic recurrence solution to the Smoluchowski equation which allows, in principle, the generation of the entire cluster size distribution from the partial distribution given by the Monte-Carlo code.

I. INTRODUCTION

The method that is presented here has its inspiration in the desire to compute the internal structure as well as the cluster size spectrum of clusters that have coagulated from a chemically nonhomogeneous, monodisperse medium. This problem occurs frequently in many fields ranging from meteorology, where the computation of nucleation rates for acidic water droplets can be applied to the problems of smog and acid rain formation, to astrophysics, where the process of dust formation in stellar environments plays an important role in understanding the dynamics and evolution of the interstellar medium.

Whenever a new method is developed to investigate a complicated dynamic system, some simplifications are usually necessary to make the problem more tractable to solution. In this paper it has been assumed that the medium is chemically homogeneous and that particles stick together whenever they collide. The problem of nucleation is then avoided and the program becomes more applicable to solving the Smoluchowski equation (see Eq. (13)). Binning methods are the basis for most routines that obtain solutions to the Smoluchowski equation. This is due to the large range in scales that is inherent in cluster formation. Since a one micron particle can easily contain over 10^9 atoms and it is currently impossible to store all this information efficiently, one is forced to bin the clusters into a number of different size ranges. Although the use of this method has produced profound results, it does not lead to a simple way of investigating the internal structure of the clusters, which is one of the final aims (although unfulfilled in this paper) of this research.

One natural approach to this problem is to use the Monte-Carlo method to simulate the aggregation of clusters from gaseous material. This is done by observing the individual behavior of particles in a large reservoir of (initially) gaseous material as it develops with time. Of course the number of particles in a gaseous medium can easily be of order 10^{23} or higher and it is impossible to monitor the behavior of each particle individually, so a sample of 10^5 randomly distributed test particles are chosen and it is assumed that their subsequent behavior is an indicator of the behavior of the medium as a whole (Fig. 1a). Such an assumption may be tested by comparing the direct simulation Monte-Carlo (DSMC) results with the three known analytic solutions to the Smoluchowski equation. In all such comparisons, the DSMC results are found to reproduce the expected distributions within the tolerances of statistical error.

The DSMC method is able to overcome the problem of limited memory storage, because only the test particles need to be observed and since a 32-bit memory element can easily store integer numbers up to around 10^9, there is no impediment (besides computer time) in obtaining cluster sizes of physical interest. Indeed a general recursive solution to the Smoluchowski equation can be derived which, when coupled with the DSMC results, allows the computation—in principle—of the cluster size distribution to a much larger size.

II. DSMC METHODS

If a gas contains an assortment of different sized clusters, then the probability (R_i) per unit time of a cluster that contains i structural units (we call this an $\{i\}$ cluster) interacting with any other cluster excepting itself is

$$R_i = \sum_{j=1}^{\infty} n_j \sigma_{ij} \langle v_{ij} \rangle - \frac{\sigma_{ii} \langle v_{ii} \rangle}{V}, \tag{1}$$

0021-9991/92 $5.00

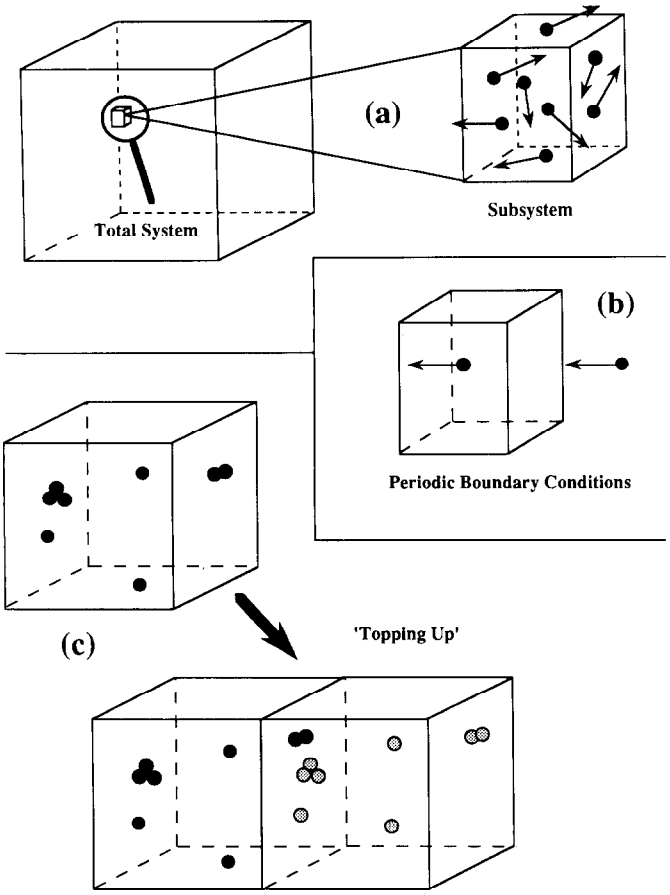

FIG. 1. (a) The Monte-Carlo code can only examine 10^4 or 10^5 particles at a time. Since a reasonably sized system of gas contains approximately 10^{23} particles, it is necessary to consider a subsystem of the total system and assume that the behavior of the subsystem duplicates the system as a whole. (b) The subsystem satisfies the constraint of periodic boundary conditions; i.e., as a particle moves out, an identical particle moves in to the system. (c) It is important that a robust number of clusters be resident in the subsystem, since the error in the simulation goes like the square root of the total cluster number. As clustering proceeds, the total number of clusters within the subsystem must decrease. When the number of clusters becomes too small, we protect against statistical fatigue by simply adding the subsystem to itself, thereby doubling the number of clusters in the subsystem.

where n_j is the number density of the $\{j\}$ species in the total system, V is the volume of the system, and σ_{ij} and $\langle v_{ij}\rangle$ is the cross sectional area of interaction and the mean relative speed, respectively, between the $\{i\}$ and $\{j\}$ species. Usually $n_j \gg 1$ and so we can make the approximation

$$R_i = \sum_{j=1}^{\infty} n_j \sigma_{ij} \langle v_{ij} \rangle. \tag{2}$$

The mean time for an $\{i\}$ cluster interacting with any other cluster (τ_i) is then

$$\tau_i = 1 \Big/ \sum_{j=1}^{\infty} n_j \sigma_{ij} \langle v_{ij} \rangle. \tag{3}$$

The direct simulation Monte-Carlo code takes a subsystem of test particles (usually 10^4 to 10^5 particles) from the reservoir of gas (Fig. 1a). Periodic boundary conditions are assumed: particles moving out of the subsystem are immediately replaced by identical particles moving into the subsystem (Fig. 1b). Let F_j denote the number density of the $\{j\}$ species for the test particles, let F_c be the total number of clusters in the subsystem, and let n_c be the total number of clusters in the total system; then we can relate the number densities of the test particle subsystem to the number densities of the total system,

$$\frac{F_j}{F_c} \approx \frac{n_j}{n_c}, \tag{4}$$

where

$$F_c = \sum_{j=1}^{\max j} F_j \quad \text{and} \quad n_c = \sum_{j=1}^{\infty} n_j. \tag{5}$$

Substituting (4) into (2) and (3) implies that

$$R_i \approx \frac{n_c}{F_c} \sum_{j=1}^{\max j} F_j \sigma_{ij} \langle v_{ij} \rangle \tag{6}$$

and

$$\tau_i \approx 1 \Big/ \frac{n_c}{F_c} \sum_{j=1}^{\max j} F_j \sigma_{ij} \langle v_{ij} \rangle. \tag{7}$$

The Monte-Carlo code examines each cluster in turn and decides whether that cluster will interact with any other cluster in the distribution. The probability of a single $\{i\}$ cluster interacting with any other cluster during a time Δt ($Pr_i(\Delta t)$) is approximately $\Delta t/2\tau_i$ or, more exactly,

$$Pr_i(\Delta t) = 1 - \exp\left(-\frac{\Delta t}{2\tau_i}\right). \tag{8}$$

The factor of two arising, because during each time step Δt the clusters are double counted and so the computed rate of interaction is twice the actual physical rate. As the system evolves, the value of τ_i will also change and it is therefore not prudent to keep a fixed Δt. To overcome this problem, Δt is made time dependent and is defined to be the minimum of all the τ_i's obtained at the previous timestep multiplied by a constant:

$$\Delta t^{\text{new}} = \alpha \min(\tau_1, \tau_2, \tau_3, \ldots, \tau_{\max t})|_{t - \Delta t^{\text{old}}}. \tag{9}$$

Accurate results are generally obtained when the multiplicative constant, α, has the value of 0.1 or less.

As is standard in Monte-Carlo simulations, if we have the condition that G—the random number generator ($G \in [0, 1]$)—is less than $Pr_i(\Delta t)$ then the $\{i\}$ cluster will stick to some other cluster. To find out with which cluster the $\{i\}$ cluster will interact, it is necessary to compute the probability of interaction between the $\{i\}$ cluster and any other cluster in the subsystem, this being simply

$$P_{ij} = \frac{F_j \sigma_{ij} \langle v_{ij} \rangle}{\sum_{j=1}^{\max j} F_j \sigma_{ij} \langle v_{ij} \rangle}. \tag{10}$$

After generating another random number G, it is possible to determine the size of the cluster with which the $\{i\}$ cluster will interact, from the condition

$$\sum_{j=1}^{k-1} P_{ij} \leqslant G \leqslant \sum_{j=1}^{k} P_{ij}, \tag{11}$$

which in this case implies that a $\{k\}$ cluster will combine with the $\{i\}$ cluster.

A schematic example illustrates how the code works. The data structures that contain the clusters are two arrays which are called "old" and "new." In Fig. 2a the first element of the "old" array contains a cluster of size 10 structural units, the second element contains a {20} cluster, and so on to the end of the array. At the start of a timestep, "new" and "old" are identical and they will remain that way if there are no interactions between the clusters. Each cluster in "old" is considered in turn and, if the probabilities computed by Eq. (8) are such that there is no interaction, then the program will go on to consider the next cluster in the array. Suppose, however, that a cluster is found which is about to interact with some other cluster.

In Fig. 2b the program has determined that the {15} cluster in array element m is just such a cluster. From Eq. (11) it is then found that the {3} cluster at position k in "old" is going to combine with the chosen {15} cluster. Corresponding clusters are located in the "new" array, where the {3} cluster is combined with the {15} cluster in "new," which leaves a {0} cluster where the {3} cluster used to be and an {18} cluster in place of the original {15} cluster (see Fig. 2c). These reactions or non-reactions are continued until the last element in "old" has been checked. The "new" array is then copied onto the "old" array and the process is repeated for the next timestep. As can be seen from Fig. 2, this method allows double counting to occur; e.g., not only can the {3} cluster interact with the {15} cluster, but it is possible that the {15} cluster will interact with the {3} cluster, since the "old" array remains unchanged during one timestep. Statistically, we account for this double coagulation via the factor of 2 in Eq. (8).

If coagulation is continued for a long time, the number of clusters in the subsystem will decrease to a point where the results will become statistically unreliable. To stop this from

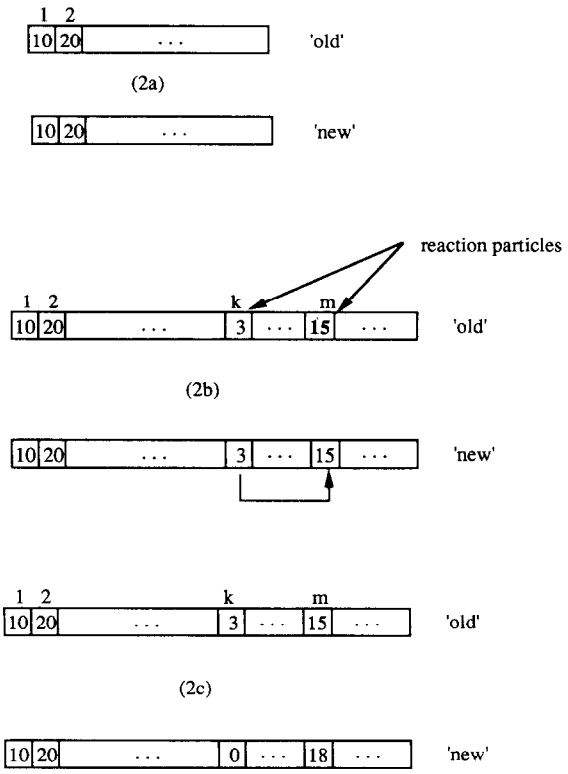

FIG. 2. Schematic portrayal of a "reaction." Two arrays called "old" and "new" are required. Initially "old" and "new" are the same (Fig. 2a), until Eq. (8) chooses the {15} cluster at array element m to be a reaction particle (Fig. 2b). The reaction partner is then found by Eq. (11) to be the {3} cluster at array elment k. Finally, in Fig. 2c the {3} cluster is combined with the {15} cluster, leaving a {0} cluster and an {18} cluster in the "new" array.

happening, new particles are allowed into the subsystem before statistical fatigue occurs. This "topping up" can be accomplished from the assumption that the subsystem simulates the behavior of the total system and so the probability of obtaining a cluster of size k (P_k) is then

$$P_k = \frac{n_k}{n_c} \approx \frac{F_k}{F_c}. \tag{12}$$

It is then a simple matter of multiplying P_k by a larger F_c, which in turn will give a larger F_k, and the program once again has a robust number of particles. Figure 1c provides a more intuitive description: here we simply double the number of particles in the subsystem, which is equivalent to adding an exact copy of the subsystem to itself. A more detailed description of this process complete with error analysis is given in Appendix B.

III. DSMC VERSUS THEORY

Naturally the DSMC method should be compared to known clustering results to determine whether it is a valid

method of analysis. In this section the validity of the method is tested by comparison with the most famous and well-studied aggregation equation: the Smoluchowski equation,

$$\frac{dn_k}{dt}=\frac{1}{2}\sum_{i=1}^{k-1}K_{i(k-i)}n_i n_{(k-i)}-n_k\sum_{i=1}^{\infty}K_{ik}n_i, \qquad (13)$$

where t is the time, K_{ij} is the kinetic coagulation kernel of the reaction, and n_k is the number density of the $\{k\}$ cluster.

The first term on the right-hand side of the Smoluchowski equation refers to the formation of the $\{k\}$ species by the reaction of the $\{i\}$ and $\{k-i\}$ species, so that $i+(k-i)=k$, the second term, keeps tab of the disappearance of the $\{k\}$ term via the creation of $\{k+i\}$ species. The one-half factor arises because one counts the same terms twice in the sum. Analytic solutions for the Smoluchowski equation have only been found for the cases $K_{ij}=A$, $K_{ij}=A(i+j)$, and $K_{ij}=A(i*j)$ (see Refs. [1–9]), where A is an arbitrary positive numerical constant. By noting that $K_{ij}n_i n_j$ is the probability per unit time per unit volume that the event $\{i\}+\{j\}=\{i+j\}$ will occur, then it can be deduced that

$$K_{ij}=\sigma_{ij}\langle v_{ij}\rangle, \qquad (14)$$

where σ_{ij} is the cross section of interaction and $\langle v_{ij}\rangle$ is the mean relative speed between an $\{i\}$ and a $\{j\}$ cluster. Using (14) we now can relate the DSMC method developed in Section II to the solutions of (13), by assuming that the clusters stick together whenever they collide.

Case 1. $K_{ij}=A$. If we define n as the number of structural units or atoms in the total system then the analytic solution (which was first obtained by Smoluchowski [6]) of Eq. (13) for the initial condition $n_1=n$ (or $n_c(t=0)=n$) and the case $K_{ij}=A$ is

$$n_k=n\frac{(nAt/2)^{k-1}}{(1+nAt/2)^{k+1}}. \qquad (15)$$

From Eq. (15) one can show:

$$\sum_{k=1}^{\infty}n_k=\frac{n}{1+nAt/2}. \qquad (16)$$

So the probability of obtaining a cluster containing k atoms (P_k) is

$$P_k=\frac{n_k}{\sum_{k=1}^{\infty}n_k}=\frac{(nAt/2)^{k-1}}{(1+nAt/2)^k}. \qquad (17)$$

Defining θ to be the ratio of the number of structural units to the number of clusters gives

$$\Theta(t)=\frac{n}{n_c}=1+\frac{nAt}{2}. \qquad (18)$$

Placing $n=2.7\times10^{19}\,\mathrm{cm}^{-3}$ and $A=2/n\approx7.407\times10^{-20}\,\mathrm{cm}^3\,\mathrm{s}^{-1}$ into the DSMC code and Eq. (18) allows the construction of Fig. 3. The probability spectrum for the cluster sizes is shown in Fig. 4, where the DSMC results are plotted against the theoretical line from Eq. (17).

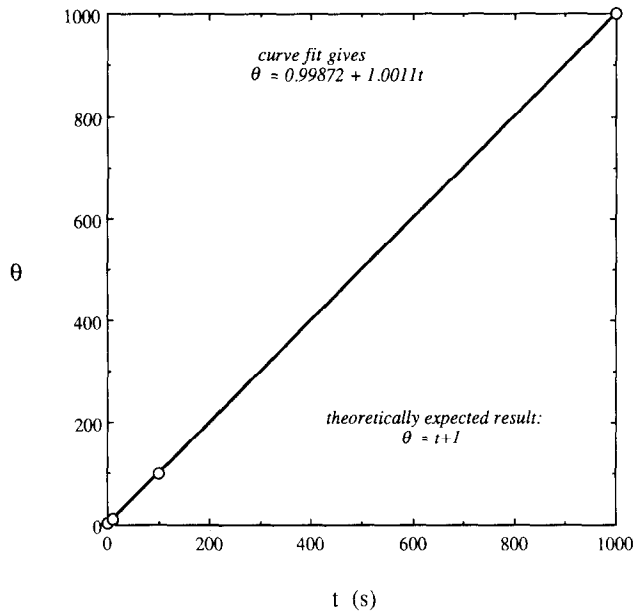

FIG. 3. The ratio of the total number of structural units to the total number of clusters (θ) as a function of time (t) for the case $K_{ij}=7.407\times10^{-20}\,\mathrm{cm}^3\,\mathrm{s}^{-1}$. Approximately 10^5 clusters exist in the sample subsystem at any one time. The total system is assumed to contain 2.7×10^{19} structural units/cm^3 at $t=0$ and at $t=1000$ s the subsystem contains 10^9 structural units. The DSMC results follow the theoretical results so closely that the line of best fit is nearly identical to the theoretical result.

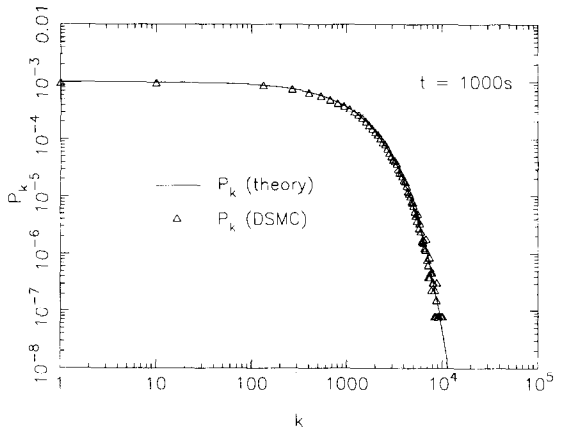

FIG. 4. The probability of obtaining a cluster containing k structural units versus the size of the clusters at $t=1000$ s. Both the theoretical line and the DSMC results are shown, where the largest cluster formed by the Monte-Carlo simulation, contains approximately 20,000 structural units.

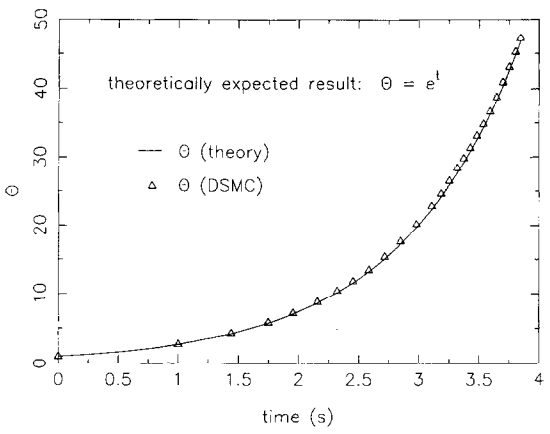

FIG. 5. The ratio of the number of structural units over the number of clusters as a function of time for the case $K_{ij}=A(i+j)$, where $A\approx 3.7\times 10^{-20}$ cm^3 s^{-1} and the initial density of the gas $=2.7\times 10^{19}$ cm^{-3}. A comparison is made between the theoretically expected results given by Eq. (20) and the results given by the DSMC code.

Case 2, $K_{ij}=A(i+j)$. The analytic solution for the Smoluchowski equation for the initial condition $n_1=n$ (or $n_c(t=0)=n$) and case $K_{ij}=A(i+j)$ (see Ref. [2]) is

$$n_k=n\frac{k^{k-1}}{k!}e^{-nAt}(1-e^{-nAt})^{k-1}e^{-k(1-e^{-nAt})}. \tag{19}$$

It can also be shown independently that

$$\Theta(t)=\frac{n}{n_c}=e^{nAt}; \tag{20}$$

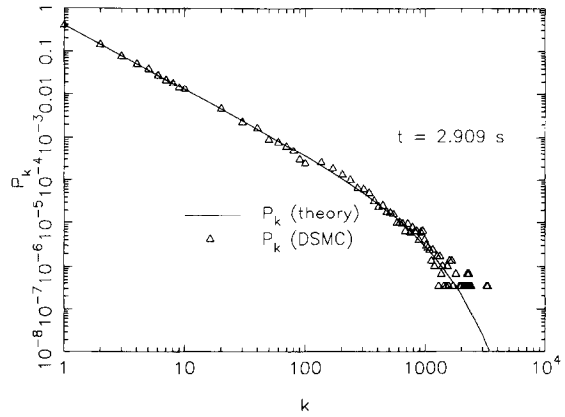

FIG. 6. The probability of obtaining a cluster containing k structural units versus the number of structural units in each cluster. The theoretical result is shown as the unbroken line, while the "experimental" results from the Monte-Carlo program are represented by open triangles. The simulation starts at time $t=0$ with a monodisperse medium (i.e., the gas consists entirely of structural units with no clusters containing two or more structural units) and the results presented here show the system at $t=2.909$ s. The set of triangles at the 3×10^{-7} level demonstrate the highly statistical nature of the simulation. As more clusters containing approximately 2000 structural units are formed, the statistical error will decrease and the simulation results will approach the theoretically expected results.

thus P_k has the form

$$P_k=\frac{n_k}{n_c}=\frac{n_k}{n}\Theta$$
$$=\frac{k^{k-1}}{k!}(1-e^{-nAt})^{k-1}e^{-k(1-e^{-nAt})}. \tag{21}$$

In this example, n is the same as in Case 1 and $A\approx 3.7\times 10^{-20}$ cm^3 s^{-1}. The comparisons between the theoretical results and the DSMC results are shown in Figs. 5 and 6.

Case 3, $K_{ij}=A(i*j)$. The theoretically predicted behavior of the solution to the Smoluchowski equation for the case $K_{ij}=A(i*j)$ is unusual, because after a finite time a supercluster or "runaway" mass is formed (see Refs. [3, 4, 7, 9, 11, 12]). The ratio of the number of structural units in the subsystem to the number of clusters in the subsystem is given by

$$\Theta(t)=1\Big/\left(1-\frac{nAt}{2}\right),\qquad 0\leqslant t<\frac{1}{nA}, \tag{22}$$

the formation of the supercluster occurring at $t=1/nA$. P_k now has the form

$$P_k=\frac{k^{k-2}}{k!}\frac{(nAt)^{k-1}}{(1-nAt/2)}e^{-knAt},\qquad 0\leqslant t<\frac{1}{nA}. \tag{23}$$

For times greater than $1/nA$, an analytic solution to the classical Smoluchowski equation is not possible. The reasons for this breakdown are discussed in [11] and will not be given here. However, a semi-analytical solution due to a modified Smoluchowski equation can be given which

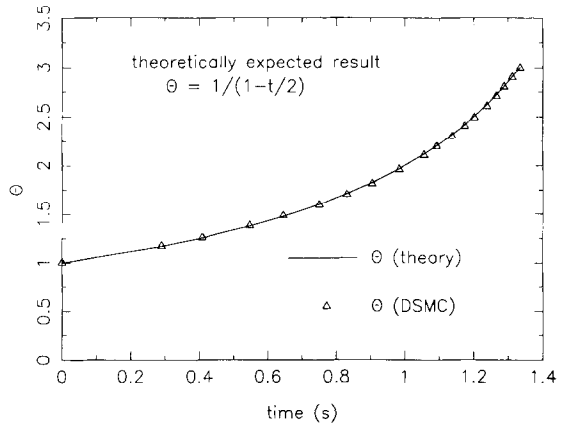

FIG. 7. The ratio of the number of structural units over the number of clusters as a function of time for the case $K_{ij}=A(i*j)$, where $A=1/n\approx 3.7\times 10^{-20}$ cm^3 s^{-1} (n—the initial density of the gas $=2.7\times 10^{19}$ cm^{-3}). A comparison is made between the theoretically expected results given by Eq. (22) and the results obtained from the DSMC code.

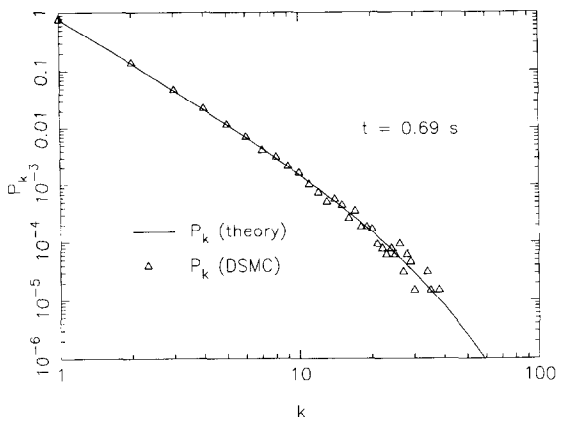

FIG. 8. The probability of obtaining a cluster containing k structural units versus the number of structural units in each cluster. The theoretical result given by Eq. (23) is shown by the line, while the "experimental" results from the DSMC program are represented by triangles. The simulation starts at time $t=0$ with a monodisperse medium and the results presented here show the system at $t=0.69$ s.

allows for the formation of a runaway cluster (see Ref. [11]). This behavior of a continuous solution suddenly changing to a continuous plus discrete solution is demonstrated by the DSMC results which are shown in Figs. 7, 8, and 9, where in this example $n=2.7\times10^{19}$ cm^{-3} and $A\approx3.7\times10^{-20}$ cm^3 s^{-1} (Therefore, $nA=1$ s^{-1}).

Figures 7 and 8 demonstrate the agreement of the theoretical and Monte-Carlo results for times less than 1 s. Figure 9 shows that for $t=1.33$ s the "small" clusters still approximately agree with Eq. (23), while—as expected—the large "Monte-Carlo" clusters have all congealed into one super cluster. This is due to the multiplicative nature of the reaction cross section: $\sigma_{ij}\propto K_{ij}$, which for times >1.0 s causes the largest cluster to dominate just about all the reactions.

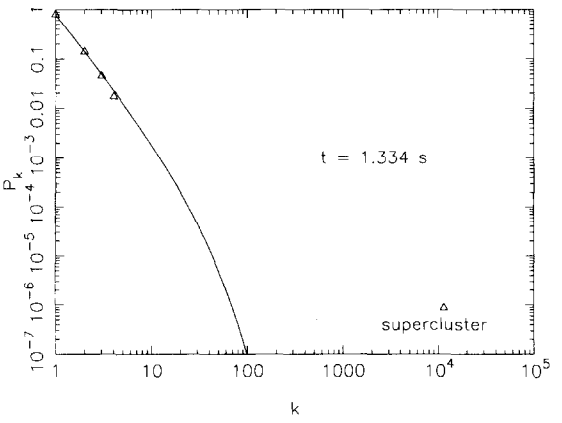

FIG. 9. As discussed in the text, when t is greater than $1/nA$ the theoretical solution given by Eq. (23) breaks down and a super cluster or gel begins to form. This behavior is illustrated in the above figure, which plots the probability of obtaining a cluster containing k structural units versus k. Interestingly, only five differently sized clusters are found to exist at $t=1.334$ s: $k=1$, 2, 3, 4, and 11,500. Also the theoretically expected values and the Monte-Carlo results agree only for $k=1$, 2, 3, and 4. The supercluster has begun to dominate the reaction and has consumed all but the smallest clusters.

IV. RECURSIVE INDUCTION

As demonstrated in Section III, one can obtain a fairly adequate cluster size spectrum from the DSMC technique. Unfortunately the extent of the size spectrum that can be mapped is a function of the number of particles that are considered in the Monte-Carlo subsystem and, as such, is limited. It would be advantageous to have a method which could derive information from the Monte-Carlo data to map out the cluster size spectrum to an arbitrarily sized cluster.

Such a process is made possible via the use of Eq. (A25) which is derived (assuming monodisperse initial conditions) in Appendix A and has the form:

$$P_k(t)=\frac{\aleph(t)}{(k-1)}\sum_{i=1}^{k-1}K_{i(k-i)}P_i(t)\,P_{k-i}(t). \tag{24}$$

The quantity $\aleph(t)$ may be expressed analytically as

$$\aleph=\left(\frac{e^{\gamma}n_c}{2A}\right)\Bigg|_{\text{Monte Carlo}} \tag{25}$$

(the terms e^{γ} and A are mathematical quantities obtained in the derivation of (24)—see Appendix A), but for computational purposes $\aleph(t)$ is determined from the Monte-Carlo results (see Eq. (A24)). Once a value for $\aleph$ is obtained we can use (24) to determine P_k from $\{P_1, P_2, P_3, ..., P_{k-1}\}$. Equation (24) is an exact general solution to the Smoluchowski equation; however, the accuracy of the solutions obtained is dependent on $\aleph$. An analysis of the error propagation is given in Appendix C; however, for this section it will suffice to consider a graphical description of the process.

Figure 10 shows a trial with the Case 2 (see Section III) coagulation kernel, $K_{ij}=A(i+j)$. At $t=0.242$ s the Monte-Carlo code has mapped out the size spectrum for clusters containing 1, 2, 3, 4, 5, 6, 7, 8, and 11 structural units. From this information, a value of $\aleph$ is obtained and P_k is calculated for $k\in\{9, 10, 12, 13, ..., 100\}$, but for ease of viewing only the values $k=9$, 10, 20, ..., 100 are shown. Also shown in Fig. 10 is the line that plots the theoretically determined solution. As can be seen from Fig. 10, there is respectable agreement between the values given by (24) and the theoretically expected values obtained from Eq. (21).

It should be emphasized, that (A24) allows the computation of P_k to magnitudes that would be impossible to compute if one were to rely on DSMC technique alone. This can be seen from Fig. 10 which shows values of P_k down to

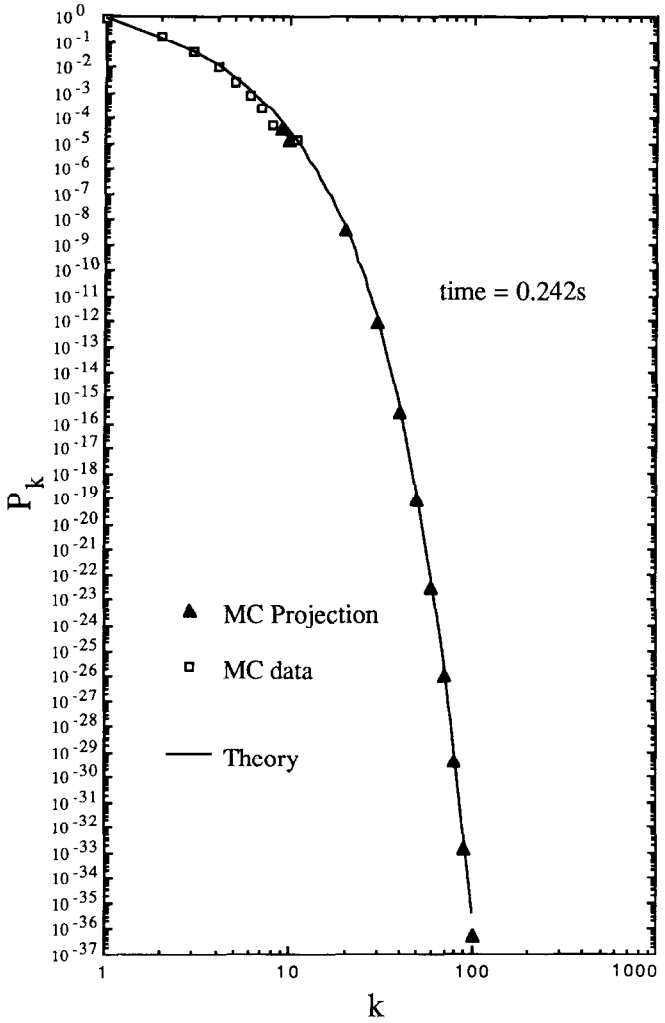

FIG. 10. P_k versus k for the Case 2 (see Section III) coagulation kernel: $K_{ij} = A(i + j)$. At $t = 0.242$ s the Monte-Carlo code has mapped out the size spectrum for clusters containing 1, 2, 3, 4, 5, 6, 7, 8, and 11 structural units (open squares). From this information, a value of $\aleph$ is obtained and P_k is calculated via (24) for $k \in \{9, 10, 12, 13, ..., 100\}$, but for ease of viewing only the values $k = 9, 10, 20, ..., 100$ are shown (dark triangles). Also shown in Fig. 10 is the theoretically determined solution (solid line).

10^{-37}. To obtain such values from the DSMC code would require memory capacity and processing speeds far beyond those obtained by present day computers. Unfortunately, as is shown in detail in Appendix C, the rapid growth of errors in (24) limits the utility of this equation.

CONCLUSION

A method for analyzing cluster coagulation has been presented which relies on a Monte-Carlo analysis of individual particles as they interact and form clusters from a homogeneous monodisperse medium. Three case studies have been presented, which compare the DSMC results to the three known analytic solutions of the Smoluchowski equation (Eq. (13)). In all such comparisons, the DSMC results are found to reproduce the expected distributions within the tolerances of statistical error.

The kinetic coagulation kernels that allow analytic solutions to the Smoluchowski equation, $K_{ij} = A$, $K_{ij} = A(i + j)$, and $K_{ij} = A(i*j)$, usually have little relevance to problems that arise in nature. Remembering that $K_{ij} = \sigma_{ij}\langle v_{ij}\rangle$, the DSMC method should be able to handle any non-infinite functional form of $\sigma_{ij}\langle v_{ij}\rangle$. For example, a dilute Maxwellian gas, consisting of hard spheres, has $\sigma_{ij}\langle v_{ij}\rangle = A(i^{-1} + j^{-1})^{1/2}(i^{1/3} + j^{1/3})^2$. Thus with the appropriate σ_{ij} and $\langle v_{ij}\rangle$, the DSMC method can be used to tackle "real" world problems. The only limitation being that of computer time.

In the fourth case that is studied, a recursive induction technique is discussed. The technique gains its name, because it uses the Smoluchowski equation and the DSMC results to obtain P_k's for higher k's than can be obtained from the DSMC method. The recursive induction equation (Eq. (24)) is only applicable to coagulation systems for which the Smoluchowski equation is a valid description. Unfortunately, due to the build up of error, the recursive induction technique is limited to cases where less than a thousand iterations are required.

APPENDIX A: PROBABILITY RECURSION FORMULA FOR THE SMOLUCHOWSKI EQUATION

As stated in Section III the Smoluchowski equation has the form

$$\frac{dN_k}{dt} = \frac{1}{2}\sum_{i=1}^{k-1} \kappa_{i(k-i)} N_i N_{k-i} - N_k \sum_{i=1}^{\infty} \kappa_{ik} N_i, \qquad \text{(A1)}$$

where the n_k of Eq. (13) has been replaced with N_k—the number of clusters that contain k structural units $= n_k V$ and the coagulation kernel of Eq. (13): K_{ij} has been replaced by κ_{ij}, where $\kappa_{ij} = K_{ij}/V$, V being the volume of the system. N_k satisfies the constraints,

$$\sum_{k=1}^{\infty} N_k = N_c \qquad \text{(A2)}$$

$$\sum_{k=1}^{\infty} kN_k = N, \qquad \text{(A3)}$$

N_c being the total number of clusters and N is the total number of structural units in the system (N, $N_c < \infty$).

If we assume that classical statistics are appropriate for describing this system; i.e., each monomer is distinguishable, each cluster size is distinguishable, but permutations of the structural units within a cluster are ignored, then we can apply a number of state functions that were developed by Stockmayer [10].

The number of ways of producing the size distribution $(N_1, N_2, N_3, \ldots)$, given the constraints (A2) and (A3), is denoted by $\Omega(N, N_c: N_1, N_2, N_3, \ldots)$, where

$$\Omega(N, N_c: N_1, N_2, N_3, \ldots) = \frac{N!}{N_1!\, N_2!\, N_3! \cdots} \left(\frac{w_1}{1!}\right)^{N_1} \left(\frac{w_2}{2!}\right)^{N_2} \left(\frac{w_3}{3!}\right)^{N_3} \cdots, \quad \text{(A4)}$$

w_k being the number of ways of forming a $\{k\}$ cluster from k structural units (which implies that $w_1 = 1$).

A derivation of (A4) is given in [7]. From (A4) one can use Lagrange multipliers to determine the most probable cluster size distribution $(N_1^*, N_2^*, N_3^*, \ldots)$ via the auxiliary function,

$$F(N_1, N_2, N_3, \ldots) = \ln \Omega(N, N_c: N_1, N_2, N_3, \ldots) - \gamma N_c - \beta N, \quad \text{(A5)}$$

where γ and β are Lagrange multipliers. Setting $\partial F/\partial N_k$ equal to zero and using Stirling's approximation for large N_k $(\ln(N_k!) \approx N_k \ln(N_k) - N_k)$, one obtains

$$N_k^* = \frac{w_k}{k!} e^{-\gamma - \beta k}. \quad \text{(A6)}$$

Substituting (A6) into (A1) and multiplying both sides of the result by $k!\, e^{(2\gamma + \beta k)}$ gives the result

$$w_k e^{\gamma} \frac{d(-\gamma - \beta k)}{dt} = -w_k \sum_{i=1}^{\infty} \kappa_{ik} \frac{w_i}{i!} e^{-\beta i} + \frac{1}{2} \sum_{i=1}^{k-1} \binom{k}{i} \kappa_{i(k-i)} w_i w_{k-i}. \quad \text{(A7)}$$

Substituting (A6) into (A2), differentiating with respect to t, and rearranging implies

$$\frac{d(-\beta)}{dt} = \frac{1}{N}\frac{dN_c}{dt} - \frac{N_c}{N}\frac{d(-\gamma)}{dt}. \quad \text{(A8)}$$

In Eq. (A8) and all subsequent equations, we have removed the asterisk that appears on the N_k's in (A6) with the clear understanding that we are now considering the most probable values of N_k and therefore of N_c. In the derivation of (A8), we have implicitly assumed that

$$\frac{d}{dt}\left(\sum_{k=1}^{\infty} N_k\right) = \sum_{k=1}^{\infty} \frac{d(N_k)}{dt}. \quad \text{(A9)}$$

This can be shown to be true for $t \in [0, \tau_0]$, where $\tau_0 > 0$ and $\kappa_{ij} \leqslant A(i*j)$, by using the fact that

$$\sum_{k=1}^{\infty} N_k \quad \text{and} \quad \sum_{k=1}^{\infty} kN_k \quad \text{(A10)}$$

are uniformly convergent and $t \in [0, \tau_0]$ for $K_{ij} \leqslant A(i*j)$ (see [4] for a proof of this assertion).

Combining (A10) with (A1) and the Weierstrass M test, it is possible to show that

$$\sum_{k=1}^{\infty} \frac{d(N_k)}{dt} \quad \text{(A11)}$$

is uniformly convergent for $t \in [0, \tau_0]$ and $\kappa_{ij} \leqslant A(i*j)$. Now combining (A10) and (A11) we have (A9).

Using (A8) we can write

$$e^{\gamma} \frac{d(-\gamma - \beta k)}{dt} = \frac{d(e^{\gamma})}{dt}\left[\frac{kN_c}{N} - 1\right] + e^{\gamma} \frac{k}{N}\frac{dN_c}{dt}. \quad \text{(A12)}$$

Placing (A12) into (A7),

$$w_k \left[\frac{d(e^{\gamma})}{dt}\left[\frac{kN_c}{N} - 1\right] + e^{\gamma}\frac{k}{N}\frac{dN_c}{dt}\right] = -w_k \sum_{i=1}^{\infty} \kappa_{ik} \frac{w_i}{i!} e^{-\beta i} + \frac{1}{2} \sum_{i=1}^{k-1} \binom{k}{i} \kappa_{i(k-i)} w_i w_{k-i}. \quad \text{(A13)}$$

Now as $t \to 0$, then by the assumed initial conditions, $N_k \to 0\ \forall k/\{1\}$ and $N_1 \to N$; therefore,

$$N_{1|_{t=0}} = e^{-(\gamma + \beta)}|_{t=0} = N, \quad \text{(A14)}$$

$$N_{k|_{t=0}} = \frac{w_k}{k!} e^{-\gamma - \beta k}|_{t=0} = 0; \quad \text{(A15)}$$

$$\text{combining (A14) and (A15)} \Rightarrow e^{-\beta}|_{t=0} = 0; \quad \text{(A16)}$$

$$\text{this and (A14)} \Rightarrow e^{-\gamma}|_{t=0} = \infty. \quad \text{(A17)}$$

To obtain the desired equation, we require one more result:

LEMMA A1. *If* $\kappa_{ij} \leqslant A(i*j)$ *(and* $0 < A < \infty$*) then* $|dN_c/dt| < \infty$ *for* $t \in [0, \tau_0]$, $\tau_0 > 0$.

Proof.

$$\left|\frac{dN_c}{dt}\right| = \left|\sum_{k=1}^{\infty} \frac{dN_k}{dt}\right| = \left|\frac{1}{2}\sum_{k=1}^{\infty}\sum_{i=1}^{k-1} \kappa_{i(k-i)} N_i N_{k-i} - \sum_{k=1}^{\infty} N_k \sum_{i=1}^{\infty} \kappa_{ik} N_i\right| = \left|-\frac{1}{2}\sum_{k=1}^{\infty}\sum_{i=1}^{\infty} \kappa_{ik} N_i N_k\right|.$$

By assumption, $\kappa_{ij} \leqslant A(i*j)$, therefore,

$$\sum_{k=1}^{\infty}\sum_{i=1}^{\infty}\kappa_{ik}N_iN_k \leqslant A\sum_{k=1}^{\infty}\sum_{i=1}^{\infty}ikN_iN_k$$
$$= A\left(\sum_{k=1}^{\infty}iN_i\right)\left(\sum_{k=1}^{\infty}kN_k\right)$$
$$= AN^2 < \infty;$$

therefore,

$$\left|\frac{dN_c}{dt}\right| < \infty \qquad \forall t \in [0, \tau_0],$$

as required.

Using Lemma A1, (A17), and the initial condition $N_c = N$, Eq. (A10) becomes

$$(k-1)\,w_k \left.\frac{d(e^{\gamma})}{dt}\right|_{t=0} = \frac{1}{2}\sum_{i=1}^{k-1}\binom{k}{i}\kappa_{i(k-i)}w_iw_{k-i}, \qquad \text{(A18)}$$

denoting $(d(e^{\gamma})/dt)|_{t=0}$ by the symbol Λ, we have simply

$$(k-1)\,w_k\Lambda = \frac{1}{2}\sum_{i=1}^{k-1}\binom{k}{i}\kappa_{i(k-i)}w_iw_{k-i}, \qquad \text{(A19)}$$

Eq. (A19) being the fundamental equation we require to solve the Smoluchowski Equation. Multiplying both sides of (A19) by

$$\frac{e^{-\gamma-\beta k}}{k!\,(k-1)\,\Lambda} \qquad \text{(A20)}$$

gives

$$N_k = \frac{e^{\gamma}}{2(k-1)\,\Lambda}\sum_{i=1}^{k-1}\kappa_{i(k-i)}N_iN_{k-i} \qquad \text{(A21)}$$

and, noting that $P_k = N_k/N_c$, then

$$P_k = \frac{e^{\gamma}N_c}{2(k-1)\,\Lambda}\sum_{i=1}^{k-1}\kappa_{i(k-i)}P_iP_{k-i}; \qquad \text{(A22)}$$

thus if we can determine e^{γ}, Λ, N_c, and P_1 as a function of time, then we will be able to determine the cluster size spectrum by iteration $\forall k > 1$.

Let us assume that we have run a Monte-Carlo simulation and that we have a set of nonzero Monte-Carlo values for P_k: $\{P_1, P_2, P_3, ..., P_{k_{\max}}\}$, where for all $k > k_{\max}$, $P_k = 0$. It should be noted that some of the P_k may be equal to zero for some $k < k_{\max}$, since the Monte-Carlo simulation may not have produced a cluster containing that number of structural units. Therefore,

$$1 - P_1 = \sum_{k=2}^{k_{\max}}P_k$$
$$= \frac{e^{\gamma}N_c}{2\Lambda}\sum_{k=2}^{k_{\max}}\left[\frac{1}{(k-1)}\sum_{i=1}^{k-1}\kappa_{i(k-i)}P_iP_{k-i}\right] \qquad \text{(A23)}$$

$$\left(\frac{e^{\gamma}N_c}{2\Lambda}\right)\Bigg|_{\text{Monte Carlo}} = \frac{1-P_1}{\sum_{k=2}^{k_{\max}}\left[(1/(k-1))\sum_{i=1}^{k-1}\kappa_{i(k-i)}P_iP_{k-i}\right]}$$
$$= \aleph; \qquad \text{(A24)}$$

substituting (A24) into (A22) gives

$$P_k(t) = \frac{\aleph(t)}{(k-1)}\sum_{i=1}^{k-1}\kappa_{i(k-i)}P_i(t)\,P_{k-i}(t), \qquad \text{(A25)}$$

where the time dependent nature of P_k and $\aleph$ have been emphasized. Equation (A25) allows us to compute any P_k subject to the limitations of numerical error, since $\aleph$ is determined from the Monte-Carlo results and is therefore an approximation of the true value.

APPENDIX B: TOPPING UP AND ERROR ANALYSIS

As outlined in Section II, we make the assumption that our collection of Monte-Carlo clusters is but a sample of a larger population of clusters. We can then define a time-dependent discrete random variable $X(t)$, where

$$X(t) \text{ is the cluster size at time } t \qquad \text{(B1)}$$

or

$$X \equiv \begin{pmatrix} 1 & 2 \cdots m \\ p_1 & p_2 \cdots p_m \end{pmatrix}. \qquad \text{(B2)}$$

The probability that the random variable X takes the value j is then

$$P(X = j) = p_j = \frac{N_j}{N_c}, \qquad j \in [1, 2, ..., m], \qquad \text{(B3)}$$

where N_j is the number of clusters that contain j structural units and N_c is the total number of clusters in the sample. The expectation of X is

$$E(X) = \sum_{k=1}^{m}x_kp_k = \sum_{k=1}^{m}kp_k$$
$$= \frac{\sum_{k=1}^{m}kN_k}{N_c} = \frac{N}{N_c} \equiv \Theta_{\text{DSMC}}. \qquad \text{(B4)}$$

The variance has the standard form

$$\text{var}(X) = E(X^2) - (E(X))^2 = v^2 \qquad \text{(say)} \qquad \text{(B5)}$$

with

$$E(X^2) = \sum_{k=1}^{m} k^2 p_k. \qquad \text{(B6)}$$

From the central limit theorem the error in the sample of our Monte-Carlo clusters is of order $\sigma/\sqrt{N_c}$, where σ is the standard deviation of the population distribution. More exactly,

$$P\left(|\Theta_{\text{DSMC}} - \Theta_{\text{population}}| < \frac{3\sigma}{\sqrt{N_c}}\right) \approx 0.997. \qquad \text{(B7)}$$

As a specific example let us consider Case 2 in Section III, where the analytic solution to the Smoluchowski equation for the coagulation kernel $K_{ij} = A(i+j)$ is compared against the corresponding DSMC result. Here $\Theta_{\text{population}} = e^t$ (Eq. (20)) and so we can compute the relative error via the equation

$$\delta = \frac{\Theta_{\text{DSMC}} - \Theta_{\text{population}}}{\Theta_{\text{population}}} \qquad \text{(B8)}$$

and plot it as a function of time (Fig. B1). The expected relative error is of order

$$\frac{\sigma/\sqrt{N_c}}{\Theta_{\text{population}}}, \qquad \text{(B9)}$$

which from the work of Spouge [7] has the analytic form

$$\left(\frac{e^t - 1}{N_c}\right)^{1/2}. \qquad \text{(B10)}$$

Since (B10) is not very helpful in establishing an upper bound on the expected error, we simply set the expected relative error to be $1/\sqrt{N_c}$ and plot its behavior as a function of time (Fig. B1).

To account for the behavior of all the quantities shown in Fig. B1, we consider what occurs to the Monte-Carlo system when the number of particles become small (e.g., when $1/\sqrt{N_c} > 1\%$ (say)). At this point the system is "topped up"; i.e., we increase the number of clusters by some factor $\beta > 1$. In mathematical terms we have

$$N_k' = \beta N_k \qquad \forall k, \qquad \text{(B11)}$$

where N_k' is the value of N_k just after the "topping up":

$$\Rightarrow \quad N_c' = \beta N_c. \qquad \text{(B12)}$$

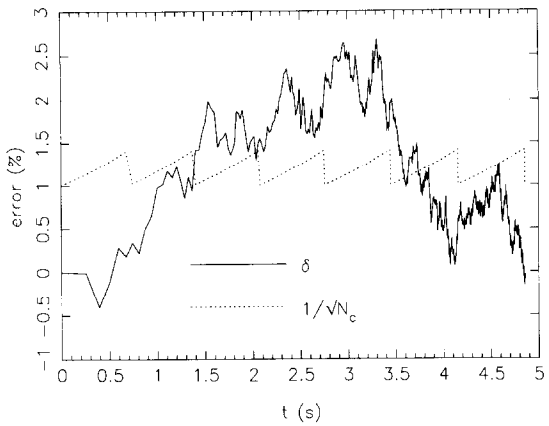

FIG. B1. Expected error ($1/\sqrt{N_c}$) and actual error (δ) as a function of time for a system of coagulating clusters with a coagulation kernel $K_{ij} = \sigma_{ij}\langle v_{ij}\rangle = A(i+j)$ ($A \approx 3.7 \times 10^{-20}$ cm^3 s^{-1} and initial density = 2.7×10^{19} cm^{-3}). The sawtooth pattern of the expected error is due to the "topping up" procedure explained in the text. As can be seen the actual error is well within the error bounds as given by Eq. (B7). The detail in the actual error curve increases with time, because the mean time of interaction (Eq. (3)) decreases as the clusters grow in size.

All the examples in this paper have used the value $\beta = 2$. So if the Monte-Carlo sample initially contains 10,000 particles, it will continue coagulating clusters until the system contains 5000 clusters, at which point all the cluster numbers will be multiplied by 2, bringing the total number of clusters back to 10,000. We can think of this as simply increasing the volume of our subsystem by the factor β, with the implicit assumption that the particles outside the subsystem are behaving in exactly the same manner as those inside the system. It is easily shown that the $E(X)$ and $\text{var}(X)$ are unchanged by such an operation.

This multiplicative factor of β explains the jump in the "sawtooth" behavior of $1/\sqrt{N_c}$. The regularity of the period between the jumps can be understood by considering Eq. (20) which shows that

$$N_c(t) = N(0)\, e^{-t}. \qquad \text{(B13)}$$

Thus the "half-life" of N_c is approximately 0.7 s, which is the period between the jumps as shown in Fig. B1.

Turning to the actual error, we see that it always satisfies the condition

$$\delta < 2/\sqrt{N_c}. \qquad \text{(B14)}$$

Indeed as time increases, the error at first increases and then decreases. Also the fluctuations increase with time, because the meantime of interaction and the timestep (as given by Eqs. (7) and (9), respectively) decrease as the clusters increase in size. Finally, the topping-up procedure does appear to increase the error at least for the first five cycles,

after which the error decreases, perhaps due to the decrease in the timestep.

APPENDIX C: ERRORS AND RECURSIVE INDUCTION

The recursive induction equation has the form:

$$P_k(t)=\frac{\aleph(t)}{(k-1)}\sum_{i=1}^{k-1}K_{i(k-i)}P_i(t)\,P_{k-i}(t). \qquad \text{(C1)}$$

To provide a simple analysis of error propagation in Eq. (C1), we require the following two assumptions plus a lemma:

(1) The error is contained in the $\aleph$ term, where $\aleph_{\text{DSMC}}=\aleph_{\text{exact}}+\Delta\aleph$.

(2) The values of P_k as obtained from the DSMC code are "exact"; i.e., their individual errors are small and can be neglected.

LEMMA C1. *Suppose the values of P_1 and $\aleph$ are known. If Eq.* (C1) *is used to determine the other values of P_k, we can write*

$$P_k=\aleph^{k-1}f_k(P_1), \qquad k\in N, \qquad \text{(C2)}$$

where

$$f_k(t)=\frac{1}{(k-1)}\sum_{i=1}^{k-1}K_{i(k-i)}f_i(t)\,f_{k-i}(t) \qquad (k>1), \qquad \text{(C3)}$$

$$f_1(P_1)=P_1. \qquad \text{(C4)}$$

Proof. Equation (C2) is certainly true for $k=1, 2, 3$. Suppose Eq. (C2) is true for all k up to $k=n-1$ $(n>1)$ then

$$\begin{aligned}P_n(t)&=\frac{\aleph}{(n-1)}\sum_{i=1}^{n-1}K_{i(n-i)}P_i(t)\,P_{n-i}(t)\\&=\frac{\aleph}{(n-1)}\sum_{i=1}^{n-1}K_{i(n-i)}\aleph^{i-1}f_i(P_1)\,\aleph^{n-i-1}f_{n-i}(P_1)\\&=\frac{\aleph^{n-1}}{(n-1)}\sum_{i=1}^{n-1}K_{i(n-i)}f_i(P_1)\,f_{n-i}(P_1)\\&=\aleph^{n-1}f_n(P_1).\end{aligned}$$

So by the principle of mathematical induction Eq. (C2) is true for all $k\in N$.

Now via the stated assumptions and Lemma (C1) we have

$$P_k=\aleph_{\text{exact}}^{k-1}\left(1+\frac{\Delta\aleph}{\aleph_{\text{exact}}}\right)^{k-1}f_k(P_1); \qquad \text{(C5)}$$

Therefore,

$$\delta P_k\equiv\frac{P_k-P_k^{\text{exact}}}{P_k^{\text{exact}}}=\left(1+\frac{\Delta\aleph}{\aleph_{\text{exact}}}\right)^{k-1}-1. \qquad \text{(C6)}$$

So if $\Delta\aleph/\aleph_{\text{exact}}=0.003$ (which is probably true for $N_c=100{,}000$) then when $k=100$, $\delta P_k\approx 0.37$; $k=1{,}000\Rightarrow\delta P_k\approx 22.5$ and finally $k=10{,}000\Rightarrow\delta P_k\approx 5.13\times 10^{13}$.

Suppose the DSMC code gives values for P_k upto some $k=m$. If we then use Eq. (C1) to compute the spectrum up to $k=n>m$, it can be shown that

$$\delta P_m\leqslant\left(1+\frac{\Delta\aleph}{\aleph_{\text{exact}}}\right)^{m-n}-1. \qquad \text{(C7)}$$

This effect can be seen in Fig. C1, where $N_c\approx 100{,}000$ and the P_k values obtained from the Monte-Carlo code have been used for $k=1$ to 400; from $k=500$ to 10,000 the P_k values have been computed via Eq. (C1). The error in the recursive iteration values is simply their vertical distance from the theoretical line. So for the $k=5000$ point the relative error, from Fig. C1, is approximately 10^6, while the expected relative error, from Eq, (C7), is $\delta P_k\leqslant 2.0\times 10^6$. This rapid growth of error thus limits the utility of Eq. (C1) to cases where the number of iterations required is in the range of 100 to 1000—such as in Section IV. Of course, if one is willing to live dangerously, it is possible to use the derived error estimates (Eqs. (C6) and (C7)) to obtain an approximation of the "correct" value for P_k.

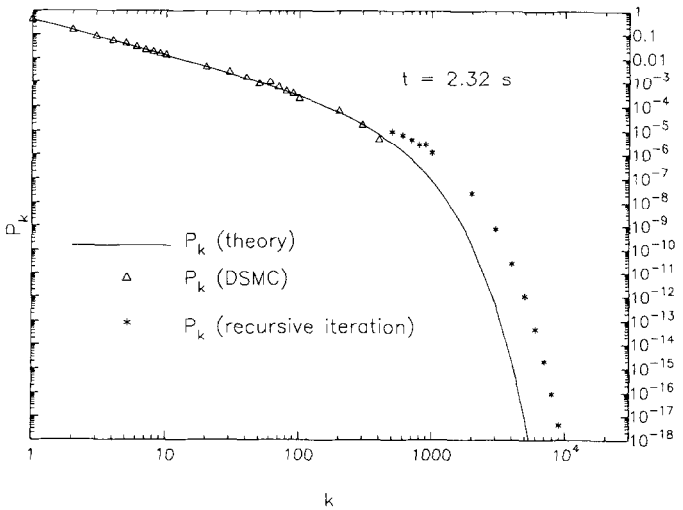

FIG. C1. P_k versus k for the Case 2 (see Section III) coagulation kernel: $K_{ij}=A(i+j)$. At $t=2.32$ s the Monte-Carlo code has mapped out the size spectrum for clusters containing 1 to 400 structural units (open triangles). From this information, a value of $\aleph$ is obtained and P_k is calculated via (C1) for $k\in\{500, 600, ..., 900, 1000, 2000, ..., 10{,}000\}$ (stars). Also shown is the theoretically determined solution (solid line). The vertical separation between the stars and the line is the error incurred from the iteration of Eq. (C1) (see the text).

ACKNOWLEDGMENTS

This work was done while the author held a National Research Council (NASA Ames Research Center) Research Associateship and it has benefited greatly from the insight and constructive criticism obtained from David C. Black, Louis J. Allamandola, Guy C. Fogleman, G. W. Wetherill, and Judith L. Huntington.

REFERENCES

1. R. L. Drake, *International Reviews in Aerosol Physics and Chemistry*, Vol. 3, edited by G. M. Hidy and J. R. Brock (Pergamon, Oxford, 1972), p. 201.
2. A. M. Golovin, *Izv. Geophys. Ser.* **5**, 482 (1963).
3. J. B. McLeod, *Q. J. Math. Oxford* **13**, 119 (1962).
4. J. B. McLeod, *Q. J. Math. Oxford* **13**, 193 (1962).
5. T. E. W. Shumann, *Q. J. R. Meteorol. Soc.* **66**, 195 (1940).
6. M. V. Smoluchowski, *Phys. Z.* **17**, 557 (1916).
7. J. L. Spouge, *Macromolecules* **16**, 12 (1983).
8. J. L. Spouge, *J. Stat. Phys.* **31** (2), 363 (1983).
9. J. L. Spouge, *J. Phys. A Math. Gen.* **16**, 767 (1983).
10. W. H. Stockmayer, *J. Chem. Phys.* **11**, 45 (1943).
11. G. W. Wetherill, *Icarus* **88**, 336 (1990).
12. R. M. Ziff, *J. Stat. Phys.* **23**, 241 (1980).